

**ON THE ORIGIN OF BIMODAL HORIZONTAL-BRANCHES
IN MASSIVE GLOBULAR CLUSTERS:
THE CASE OF NGC 6388 and NGC 6441**

Suk-Jin Yoon, Seok-Joo Joo, Chang H. Ree, Sang-Il Han, Do-Gyun Kim, and Young-Wook Lee

*Center for Space Astrophysics & Department of Astronomy, Yonsei University, Seoul
120-749, Korea*

sjyoon@galaxy.yonsei.ac.kr

ABSTRACT

Despite the efforts of the past decade, the origin of the bimodal horizontal-branch (HB) found in some globular clusters (GCs) remains a conundrum. Inspired by the discovery of multiple stellar populations in the *most massive* Galactic GC, ω Centauri, we investigate the possibility that two distinct populations may coexist and are responsible for the bimodal HBs in the *third* and *fifth* brightest GCs, NGC 6388 and NGC 6441. Using the population synthesis technique, we examine two different chemical “self-enrichment” hypotheses in which a primordial GC was sufficiently massive to contain two or more distinct populations as suggested by the populations found in ω Cen: (1) the age-metallicity relation scenario in which two populations with different metallicity and age coexist, following an internal age-metallicity relation, and (2) the super-helium-rich scenario in which GCs contain a certain fraction of helium-enhanced stars, for instance, the second generation stars formed from the helium-enriched ejecta of the first. The comparative study indicates that the detailed color-magnitude diagram morphologies and the properties of the RR Lyrae variables in NGC 6388 and NGC 6441 support the latter scenario; i.e., the model which assumes a minor fraction ($\sim 15\%$) of helium-excess ($Y \simeq 0.3$) stars. The results suggest that helium content is the main driver behind the HB bimodality found most often in massive GCs. If confirmed, the GC-to-GC variation of helium abundance should be considered a *local* effect, further supporting the argument that age is the *global* second parameter of HB morphology.

Subject headings: Galaxy: formation — globular clusters: general — globular clusters: individual (NGC 6388, NGC 6441) — stars: horizontal-branch — stars: RR Lyrae variables

1. INTRODUCTION

The horizontal-branch (HB) morphology of a globular cluster (GC) is defined as the color distribution of its HB stars. The physical cause of the wide diversity in the HB morphology among GCs with similar metallicity, or the “second parameter effect”, has long been the subject of examination (Lee, Demarque, & Zinn 1994; Stetson et al. 1996; Sarajedini et al. 1997; Lee et al. 1999a; Bellazzini et al. 2001; Catelan 2005; Recio-Blanco et al. 2006). Although several other variables may simultaneously play roles in HB morphology, the idea that GC age is the major second parameter has been very popular (Lee, Demarque, & Zinn 1994; Rey et al. 2001; Yoon & Lee 2002). However, one of the strongest arguments against the age hypothesis has been the existence of a number of GCs whose HB color distribution is distinctly bimodal (Rood et al. 1993; Stetson et al. 1996). An explanation based purely upon age as the second parameter suggests that, at a given metallicity, the population associated with the red HB is a few gigayears younger than that associated with the blue HB. This cannot be reconciled with the traditional “single-population” picture of GCs.

Perhaps the most striking examples of HB bimodality are the two Galactic bulge GCs, NGC 6388 and NGC 6441, along with NGC 2808 (Piotto et al. 2002; Sosin et al. 1997). NGC 6388 and NGC 6441 are relatively metal-rich GCs with $[\text{Fe}/\text{H}] = -0.60$ and -0.53 , respectively (Armandroff & Zinn 1998). Observations from the *Hubble Space Telescope* (*HST*) have revealed the presence of a significant fraction of extended blue-HB stars (Piotto et al. 1997; Rich et al. 1997; Pritzl et al. 2003; Piotto et al. 2002; Busso, Piotto, & Cassisi 2004; Catelan et al. 2006), in addition to a majority of red-HB stars as would be expected given their metallicity.

Recent studies suggest that the long-standing puzzle of the HB bimodality may no longer be a complete mystery. It has been discovered that at least four discrete populations coexist in the most massive Galactic GC, ω Cen (Lee et al. 1999b; Standford et al. 2006, and references therein). This finding obviously opposes the conventional “single-population” picture of GCs, and also provides an instructive precedent for the bimodal-HB feature in other GCs. The multiple populations in ω Cen imply an internal age-metallicity relation (AMR), in that stars having a higher metallicity are younger. Furthermore, subsequent

observations have revealed the presence of a marked double main-sequence (MS) with a minority population of bluer and/or fainter MS stars, which are separated from the majority (Anderson 2002; Bedin et al. 2004). Norris (2004) and Piotto et al. (2005) have suggested that a greatly enhanced helium abundance ($\Delta Y = 0.12 \sim 0.14$) can explain the split MS of ω Cen. Lee et al. (2005) have further shown that the helium-enhanced population in the MS is most likely the progenitor of the extreme HB (EHB) stars.

It has also come to our attention that the integrated luminosities of NGC 6388 and NGC 6441 (Harris 1996) make them *the third and fifth brightest* GCs next to ω Cen and M54 among the ~ 150 Galactic GCs (Yoon, Lee, & Lee 2000; Ree et al. 2002). We are particularly inspired by the fact that five of the 10 brightest GCs can be characterized by the “composite” nature of color-magnitude diagrams (CMDs), such as multiple red-giant-branches (RGBs) and/or bimodal HBs (van den Bergh 1996). The five GCs in this group are ω Cen, M54 (Siegel et al. 2007), the two GCs of interest in this study, NGC 6388 and NGC 6441, and the seventh brightest GC, NGC 2808 (Table 1, 6th column). On the other hand, according to the Harris (1996) catalog, the 11 confirmed or suspected bimodal-HB GCs (Catelan et al. 1998) are always brighter than the turnover of the V -band luminosity function ($M_V^{tot} \simeq -7$) of the Galactic GC system (Fig. 1a). The relative fraction of the combined sample of the bimodal-HB GCs, ω Cen, and M54 progressively increases at the higher brightness bin (Fig. 1b). It may be that there is a link between the massive bimodal-HB GCs and the most massive multiple-population GCs – ω Cen and M54.

The purpose of this paper is to explore, with the stellar population synthesis technique, the possibility that two distinct stellar populations may coexist and be responsible for the HB bimodality in NGC 6388 and NGC 6441. We assume the two chemical “self-enrichment” processes that were proposed to explain discrete subpopulations in ω Cen: (1) the two hypothetical subpopulations in NGC 6388 and NGC 6441 follow an internal AMR (hereafter “the AMR scenario”), and (2) NGC 6388 and NGC 6441 contain a certain fraction of super-helium-rich (SHR) stars (hereafter “the SHR scenario”). Further investigation is in progress to determine whether one of these scenarios can account for other GCs thought to contain bimodal HBs (Catelan et al. 1998), including NGC 1851, NGC 2808, and NGC 6229.

The paper is organized as follows. A brief description of the stellar population models is given in §2. We compare the synthetic CMDs (§3) and the model RR Lyraes (§4) to observed data. We argue that the bimodality of HBs and the unusual properties of the RR Lyrae variables observed in NGC 6388 and NGC 6441 are better explained by the SHR scenario. Finally, we discuss the implications of our results in §5.

2. STELLAR POPULATION MODELS

The present models are constructed using the Yonsei Evolutionary Population Synthesis (YEPS) code (Park & Lee 1997; Lee et al. 1999b; Lee, Yoon & Lee 2000; Rey et al. 2001; Yoon & Lee 2002; Lee et al. 2005; Yoon, Yi, & Lee 2006). The models use a set of stellar libraries for the MS–RGB and post-RGB evolutionary tracks that were built using the same input physics for consistency. Combined with RR Lyrae pulsation theories, the synthetic population models can predict the properties of the RR Lyrae variables (Lee, Demarque, & Zinn 1990; Yoon & Lee 2002). It is not our intention to discuss the population synthesis technique in this paper, and readers are referred to the above papers and Yoon et al. (2008, *in prep.*) for the details of the YEPS model. Table 2 and Table 3 summarize the model’s ingredients and input parameters employed in this study.

3. COLOR-MAGNITUDE DIAGRAMS

3.1. The Age-Metallicity Relation (AMR) Model

Figure 2 compares our population models to the observed *HST* CMDs of NGC 6388 and NGC 6441 (Rich et al. 1997). We note that more recent *HST* CMDs now exist for the GCs (Pritzl et al. 2003; Catelan et al. 2006). For NGC 6441, however, we selected Rich et al.’s CMD instead of that of Pritzl et al. (2003) as the former is better fit for the purposes of our CMD analysis in this section. The snapshot study by Pritzl et al. is abundant in information on variable stars and clearly more appropriate for the RR Lyrae analysis, so we fully exploit their results in §4. For the sake of consistency with the case of NGC 6441, we also opt for Rich et al.’s CMD over the superseding CMD by Catelan et al. (2006) for NGC 6388.

To simulate CMDs based on the AMR hypothesis (Figs. 2*b* & 2*e*), we first generate model CMDs assuming a common age of 13 Gyr, but different $[\text{Fe}/\text{H}]$ of -0.60 for NGC 6388 and -0.53 for NGC 6441. Once the model shows reasonable agreement with the MS through the RGB and *red* portions of the HB, we then, according to our working hypothesis, add the second minor component following a mild internal AMR. We adjust the AMR parameters until the model CMDs mimic both the overall appearance and the population number ratios of the HB. Given the level of photometric accuracy, the purpose of our CMD fit is neither to determine the absolute age of the GCs nor to make a definitive statement about their exact AMR parameters. For a direct comparison with observations, we carried out Monte Carlo error simulations based on the actual observational uncertainties.

The occurrence of a rather strong differential reddening across the fields of NGC 6388 and NGC 6441 is a well-known phenomenon (Piotto et al. 1997; Heitsch & Richtler 1999; Layden et al. 1999; Raimondo et al. 2002; Law et al. 2003). Interestingly, the differential reddening effect facilitates the development of markedly sloped red clumps. By including such an effect, our model can reproduce the tilted red clump found in the GCs. However, several studies have argued that the observed differential reddening would not be enough to turn a “normal” red HB into a significantly sloped structure (Catelan & de Freitas Pacheco 1996; Beaulieu et al. 2001; Raimondo et al. 2002). It is thus important to assess the extent to which the models are able to reproduce the red clumps.

Figure 3 illustrates our numerical experiments on the impact of differential reddening upon these structures. The middle panels (Figs. 3*b* & 3*e*) show the flat red clumps without differential reddening, and the right panels (Figs. 3*c* & 3*f*) show the tilt of the clumps due to this effect. The simulations suggest that a differential reddening value of $\sigma_{E(B-V)} = 0.03$ (mag.) is sufficient for the models to reproduce the observed tilt of the red clumps. This is comparable to the observed value of $\Delta E(B-V) < 0.1$ ($\sim 3 \times \sigma_{E(B-V)}$) in Raimondo et al. (2002), and slightly smaller than $\Delta E(B-V) \simeq 0.15$ ($\sim 5 \times \sigma_{E(B-V)}$) in Piotto et al. (1997), Heitsch & Richtler (1999), Layden et al. (1999), and Law et al. (2003). Figure 3 also shows that the models reproduce the observed RGB bump positions. It should be stressed that, in addition to the shape of red HB clumps, the differential reddening effect seems to be necessary to reproduce the observed scatter and possible tilt of the RGB bumps.

We now turn back to Figure 2. The comparison of the CMDs between observed data (Figs. 2*a* & 2*d*) and the models (Figs. 2*b* & 2*e*) shows reasonable matches from the MS through the HB. The colors of RGB stars are sensitive to metallicity, especially in the high-[Fe/H] regime. Yet, the metallicity differences between the two hypothetical populations are small enough to produce apparently single RGBs within observational uncertainties. Decreasing age shifts the color of the RGB towards blue, and this effect, albeit small, also helps to generate the single RGBs.

Another important result illustrated in Figure 2 is that the observed bimodal HBs can be reproduced by the sum of the red HB (from the metal-rich younger component) and the blue HB (from the metal-poor older component). Interestingly, theories of stellar evolution predict that increasing age or decreasing metallicity yields a bluer HB, whereas decreasing age or increasing metallicity produces a redder HB (Lee, Demarque, & Zinn 1994). Hence, it is obvious that an internal AMR splits readily the HB of each population in two, leading to bimodal HBs. Moreover, our population models (Lee et al. 1999a; Rey et al. 2001; Yoon & Lee 2002) show that the HB morphology is more sensitive to GC age by a factor of two when compared to earlier studies (Lee, Demarque, & Zinn 1994). This results in a

substantial reduction in the required age difference between blue- and red-HB populations. This is significant because all of the bimodal-HB GCs found to date (Catelan et al. 1998) have no noticeable structure in the CMDs near the MS turn-offs (Piotto et al. 2002), thus leaving little room for an age spread of more than a couple of gigayears. The difference in $[\text{Fe}/\text{H}]$ and the ages required to reproduce their CMD morphologies are 0.35 dex and 2.0 Gyr for NGC 6388, and 0.22 dex and 2.0 Gyr for NGC 6441 (Table 3).

There are several versions of the semi-empirical mass-loss formula used for reproducing the observed amount of the mass loss in giant stars. Various mass-loss formulae are summarized by Catelan (2000, 2005). We note that a different choice of formulae somewhat alters the required difference in $[\text{Fe}/\text{H}]$ and age between the blue and red HBs, but does not affect our conclusion. For instance, according to Figure 11 of Catelan (2000), the Reimers (1975) formula would allow $\Delta\text{age} = 2.0$ Gyr centered at 13 Gyr to yield a 5 % difference in ΔM (i.e., the mass loss along the RGB). If one adopts Equation A5 (the steepest one) in Catelan (2000), then 5 % in ΔM translates into $\Delta\text{age} = 2.3$ Gyr centered at 13 Gyr. Thus, even the most extreme choice of the mass-loss formula would cause only a ~ 15 % [= (2.3–2.0)/2.0] change in the age difference between red- and blue-HB populations. In order to inspect the metallicity dependence of the formulae, we take the steepest example in Figure 4 of Catelan (2005) instead of the Reimers’ formula, and find that the required difference in $[\text{Fe}/\text{H}]$ between red- and blue-HB populations in the AMR model becomes smaller by about a factor of eight. This makes the reproduction of bimodal HBs even easier.

The above analyses lead us to conclude that a mild internal AMR between the two hypothetical populations may be a plausible cause of the HB bimodality, together with the single MSs and RGBs within observational uncertainties.

3.2. The Super-Helium-Rich (SHR) Model

We now consider the SHR hypothesis. The model CMDs in Figures 2c & 2f are constructed based on this assumption. To simulate the CMDs, we adopt $[\text{Fe}/\text{H}] = -0.60$ for NGC 6388 and -0.53 for NGC 6441, with a common age of 13 Gyr and a helium abundance of $Y = 0.245$. The major dominant populations are the same in both the AMR (the metal-rich younger component denoted by “1” in Figs. 2b & 2e) and the SHR (the normal-helium component denoted again by “1” in Fig. 2c & 2f) models. We then add a helium-enhanced population according to our working hypothesis. The helium abundance and the number of stars are adjusted until the best match between the modeled and observed CMDs is achieved, especially for the blue HB appearance. Observational errors and differential reddening effects are also simulated in the same manner as in the AMR model.

Piotto et al. (2005) report that the stars of the bluer component of the split MS in ω Cen are more metal-rich (by 0.3 dex in $[\text{Fe}/\text{H}]$) than those of the dominant redder component. For NGC 6388 and NGC 6441, however, there is no such constraint dictated by observations. For a reference, in order for a 0.3 dex more metal-rich population to mimic the observed blue-HB structure in NGC 6388 and NGC 6441, the required increase in helium abundance (ΔY) is as small as 0.02. Hence, in the SHR scenario, we consider the helium-enriched population to have the same $[\text{Fe}/\text{H}]$ as the normal-Y population. The parameters required to reproduce their CMD morphologies are listed in Table 3.

The model CMDs based on the SHR assumption match well with observations from the MS through the HB. The variation in helium abundance has a relatively weak effect on the MS to the RGB, so the simulations show no indication of bifurcation on the MS through the RGB in each model CMD. The multiple MS feature, as found in ω Cen (Piotto et al. 2005) and NGC 2808 (Piotto et al. 2007), is not feasible in the available CMDs which contain considerable observational uncertainty under the MS turnoffs. More importantly, the observed bimodal HBs can be reproduced by the sum of the red HB (from the normal helium component) and the blue HB (from the helium-enriched component). For identical values of the total mass and helium core mass, theoretical models show that the HB stars with a higher Y are bluer (Rood et al. 1970; Sweigart & Gross 1976). Moreover, for a given age and metal abundance, a helium-enriched HB star has a thinner hydrogen envelope surrounding the helium-burning core, making the HB even bluer. As a result, bimodal HBs with single RGBs can be achieved given the assumption that $\sim 15\%$ of the stars in NGC 6388 and NGC 6441 have an enhanced helium abundance of $\Delta Y \simeq 0.05$ (Table 3).

The CMD morphology analysis suggests that both the AMR and SHR models are generally in first-order agreement with observations, reproducing the bimodal HBs along with the single RGBs. We proceed to make a detailed comparison of the HB structures in the two models.

3.3. Comparison between the AMR and SHR Models

Apart from the overall agreement in the CMD morphology between the observations and the models, there is an important feature of HBs that must be explained in detail. The observed HBs seem to slope upward with decreasing $(B - V)$, and their upper parts are brighter than the bulk of the red HBs by ~ 0.5 mag in V (Rich et al. 1997; Sweigart & Catelan 1998; Raimondo et al. 2002; Pritzl et al. 2003; Catelan et al. 2006).

The AMR models in Figures 2*b* & 2*e* can only partially recreate the feature by virtue of

the HB evolutionary effect (Lee, Demarque, & Zinn 1990). If there are two HB populations as predicted by the AMR model, the stars at the top of the blue HB are most likely to be highly evolved and thus brighter than stars near the zero-age HB (ZAHB). As a result, the HB evolutionary effect promotes the difference in brightness between the upper part of the blue HB and the red clump. However, inspection of Figures 2a & 2d suggests that the RR Lyraes in NGC 6388 and NGC 6441 appear to be dominated by stars near the ZAHB. It is therefore unlikely that the brightness of the blue HBs of NGC 6388 and NGC 6441 support the AMR scenario.

In contrast to the AMR model, the interesting HB appearance can be more readily reproduced by the SHR model (Figs. 2c & 2f), because helium-rich HB stars are intrinsically brighter. In an attempt to explain the sloping blue HB extensions in NGC 6388 and NGC 6441, Sweigart & Catelan (1998) have first proposed a high helium abundance ($Y \simeq 0.4$). However, Layden et al. (1999) claimed that the estimated Y values of NGC 6388 and NGC 6441 via the R-method strongly disfavor that scenario. Layden et al. showed that the models in which $Y = 0.38$ and 0.43 , presented in Sweigart & Catelan, inevitably yield $R = 3.4$ and 3.9 . These are about 3σ away from the observed value of $R = 1.6 \pm 0.7$, which corresponds to $Y = 0.25^{+0.05}_{-0.08}$. Although our SHR model in this study assumes a subpopulation with a high helium abundance ($Y \simeq 0.3$), its number fraction is as low as $\sim 15 \%$. A calculation shows that the number-weighted *mean* Y of the GCs in our SHR model is as low as $Y \simeq 0.254$ for NGC 6488 and 0.252 for NGC 6441, in complete accordance with $0.25^{+0.05}_{-0.08}$ by Layden et al. (1999).

Observations indicate that NGC 6388 and NGC 6441 contain a small portion of additional EHB stars on their HBs. For the AMR model to reproduce this detail, it should employ a unreasonably large mass dispersion ($\sigma_M \sim 0.06 M_\odot$) on the blue HBs. This is three times larger than the commonly used value of $\sigma_M = 0.02 M_\odot$ (Lee, Demarque, & Zinn 1994; Catelan et al. 1998; Yoon & Lee 2002), which is currently used for the red HBs in our models. In contrast, the SHR model requires only $\sigma_M \simeq 0.03 M_\odot$ to simulate the EHB structure. This is because, for larger helium abundances, the blue loops in the evolutionary tracks can become considerably longer, reaching higher effective temperatures (Sweigart 1987).

Alternatively, there is a possibility of the presence of a minor third subpopulation which is responsible for the EHBs in NGC 6388 and NGC 6441. In the AMR hypothesis, the third population presumably has an older age than the underlying metal-poor old population. Our model suggests an age as high as $\gtrsim 17$ Gyr. Such an unrealistically old age would not be acceptable. In the SHR model, on the other hand, the third population should have a larger ΔY than the blue-HB component. Our present model gives a helium abundance of $Y \simeq 0.33 - 0.34$ for the EHB stars in NGC 6388 and NGC 6441.

It is interesting to note that the SHR scenario is more consistent with EHB (a. k. a. “blue hook”) stars that are known to be fainter than the redder HB stars and below the ZAHB locus. Lee et al. (2005) show that the hottest EHB stars found in NGC 2808 (Brown et al. 2001) are fainter than the redder HB stars as a natural consequence of their high Y , consistent with Sweigart (1987) predictions. This may indicate that a high Y is sufficient *per se* to explain the hottest blue-hook stars without necessarily invoking a delayed helium flash (Lanz et al. 2004; Moehler et al. 2004). Readers are referred to Catelan (2005) for various characteristics of EHB stars. The origin of EHB stars and their possible link to the HB bimodality are interesting issues worth further investigation. In this study we consider the EHB stars as blue HB stars when calculating the number ratios of blue and red HB stars.

Clementini et al. (2005) have shown that the mean metallicity of the RR Lyrae stars in NGC 6441 is close enough to the typical metal abundance for this cluster. More recently, Gratton et al. (2007) have found no clear sign of star-to-star Fe abundance variation in NGC 6441 from the Giraffe spectrograph at VLT2. Hence, there appears to be a growing body of evidence that contradicts the notion that RR Lyraes and blue HB stars have a lower metal abundance. Moreover, Moehler & Sweigart (2006) have reported that the physical parameters of the cool blue HB stars in NGC 6388 are consistent with the predictions of the helium enrichment scenario, adding support to the SHR hypothesis.

We have compared the AMR and SHR models in terms of the CMD morphology, and concluded that the SHR model is more successful at reproducing the details of the observed CMDs of NGC 6388 and NGC 6441. There is yet another important feature to be accounted for – their unusual RR Lyrae properties. This is the subject of the following section.

4. RR LYRAE VARIABLE STARS

Observations (Sweigart & Catelan 1998; Layden et al. 1999; Clement et al. 2001; Pritzl et al. 2000, 2001, 2002, 2003; Corwin et al. 2006) have revealed unusual properties of the RR Lyrae variables in NGC 6388 and NGC 6441. First, the mean pulsation periods of both the *ab*- and *c*-type variables are too long for their metallicities, so they do not fall into either of the usual Oosterhoff groups (Oosterhoff 1939; Yoon & Lee 2002). Second, the number fraction of type *c* variables, $N(c)/N(ab+c)$, falls between the two Oosterhoff groups, but closer to that of the group II than of the group I. This is unusual because the traditional group II GCs are always metal-poor ($[Fe/H] \leq -1.6$). These findings have posed yet another serious challenge to our understanding of the GC stellar population. It is interesting to see whether the present models based on the AMR and the SHR hypotheses reproduce the peculiar properties of RR

Lyrae variables in NGC 6388 and NGC 6441.

4.1. The Pulsating Periods

Figure 4 presents a direct comparison between the observed and predicted RR Lyraes in NGC 6388 and NGC 6441 in terms of their pulsating periods as a function of $(B - V)_0$. In Figures 4a & 4d, we show 12 RR Lyraes found in NGC 6388 (Pritzl et al. 2002), and 63 RR Lyraes in NGC 6441 (Pritzl et al. 2001, 2003). To obtain the fundamental periods (P_F), the c -type period (P_c) has been fundamentalized using the equation, $\text{Log } P_F = \text{Log } P_c + 0.13$ (Castellani & Quarta 1987; Lee, Demarque, & Zinn 1990). As shown in Figure 2, the RR Lyrae stars are predicted to belong to the blue-HB components in both the AMR and SHR models. Since the inferred physical parameters of the blue-HB populations of NGC 6388 and NGC 6441 are almost identical (Table 3), one may consider the RR Lyrae populations of the two GCs to be twins. Indeed, Figure 4a reveals that, despite a difference in the observed number of RR Lyraes in NGC 6388 and NGC 6441, their RR Lyrae distributions in the P_F vs. $(B - V)_0$ diagram are statistically indistinguishable from each other. On these grounds, we combine the catalogs of NGC 6388 (12 RR Lyraes) and NGC 6441 (63 RR Lyraes) in order to minimize the small number statistics.

The AMR model predicts shorter periods at a given $(B - V)_0$ than observations show. Figures 4b & 4e show examples of the Monte Carlo simulations. The 10,000 Monte Carlo realizations under the AMR assumption give $\langle P_F \rangle = 0.555 \pm 0.041$ (day) from 12 ± 3 model RR Lyraes (NGC 6388) and 0.567 ± 0.017 (day) from 63 ± 7 (NGC 6441). Each of the $\langle P_F \rangle$ values is 2.6σ and 5.5σ from the observed value of $\langle P_F \rangle = 0.661$ (day) for the combined NGC 6388 and NGC 6441 data. For the AMR model to achieve a longer mean period, more highly-evolved RR Lyraes and thus a bluer HB are required. However, the number of these evolved and bright RR Lyrae stars is expected to decrease sharply as the HB morphology gets bluer. This problem has been investigated in detail by Pritzl et al. (2002), who concluded that the model, which produces the observed ratio between blue HB stars and RR Lyraes, cannot reproduce the exceedingly long mean period of NGC 6388. Therefore, the AMR model appears to be in conflict with the available RR Lyrae observations.

On the contrary, the SHR model appears to succeed in reproducing both the mean P_F and the observed $(B - V)_0 - P_F$ correlations. Figures 4c & 4f show examples of the Monte Carlo simulations. The 10,000 Monte Carlo realizations performed under the SHR assumption give $\langle P_F \rangle = 0.629 \pm 0.041$ (day) from 12 ± 3 model RR Lyraes (NGC 6388) and 0.645 ± 0.018 (day) from 63 ± 7 (NGC 6441). Each of the $\langle P_F \rangle$ values exhibits $< 1 \sigma$ agreement with the observed value of $\langle P_F \rangle = 0.661$ (day). As in the AMR model, all of the

RR Lyraes belong to the blue-HB population in the SHR model. However, this model does not require the presence of highly evolved RR Lyraes to produce long-period RR Lyraes, as helium-enhanced RR Lyraes are intrinsically brighter and of longer periods. Since most of the RR Lyraes exist at the stage of the ZAHB, their significant numbers are also reproduced. We emphasize that $\Delta Y = 0.05$ reproduces simultaneously the peculiar RR Lyrae periods and the ratio between blue HB and RR Lyrae stars.

Pritzl et al. (2002) has attributed great importance to the presence of long-period c -type RR Lyraes in NGC 6388 and NGC 6441, which are rarely found in other GCs. The mean periods of c -type variables, $\langle P_c \rangle$, in NGC 6388 and NGC 6441 are 0.36 (day) and 0.38 (day). Note that the average $\langle P_c \rangle$ for Galactic GCs is known to be 0.33 (day), respectively. In the AMR model, the assumed c -types (i.e., $(B - V)_0 \lesssim 0.3$) are concentrated toward the ZAHB (Figs. 4b & 4e) and thus have short periods. To include evolved c -types, the blue HB component must become bluer. However, the model shows that this shift gives rise to a significant decrease in the number of RR Lyraes, as discussed by Pritzl et al. (2002). In contrast to the AMR hypothesis, a raise in $\langle P_c \rangle$ agrees with the SHR scenario. The high helium content increases the zero-point of RR Lyrae brightness, leading to c -types of longer periods (Figs. 4c & 4f).

4.2. The Oosterhoff Groups

Figure 5 shows the correlation between the mean period of type ab RR Lyraes ($\langle P_{ab} \rangle$) in GCs and their $[\text{Fe}/\text{H}]$. In Figure 5a, we display the well-known Oosterhoff dichotomy (Oosterhoff 1939), along with the unusual distribution of NGC 6388 and NGC 6441. The $\langle P_{ab} \rangle$ data are obtained from Clement et al. (2001) and Corwin et al. (2006). One can see that the Galactic GCs are mainly divided into two distinct groups according to mean period and metal abundance: Oosterhoff group I (filled squares; $\langle P_{ab} \rangle \simeq 0.55$ day, and $[\text{Fe}/\text{H}] > -1.8$) and group II (open squares; $\langle P_{ab} \rangle \simeq 0.65$ day, and $[\text{Fe}/\text{H}] < -1.6$). NGC 6388 and NGC 6441 (solid diamonds) have $\langle P_{ab} \rangle$ values of 0.676 (nine ab -types) and 0.759 (42 ab -types), respectively. Note that NGC 6388 and NGC 6441 belong to neither Oosterhoff group. It is Pritzl et al. (2000) who first showed that NGC 6388 and NGC 6441 do not fall into either of the usual Oosterhoff groups, and proposed the possibility of a new Oosterhoff class. Do NGC 6388 and NGC 6441 break down the traditional Oosterhoff classification scheme? Or, do we need to add a third class to the scheme?

The answers to these questions depend solely on our understanding of the origin of the Oosterhoff dichotomy. An explanation for the phenomenon has been put forward in the work of Lee & Zinn (1990) and Yoon & Lee (2002). In particular, Yoon & Lee (2002) have

discovered that most of the lowest-metallicity ($[\text{Fe}/\text{H}] < -2.0$) GCs display a striking planar alignment in the outer-halo of the Milky Way. The alignment, combined with evidence from kinematics and stellar population, indicates that the metal-poorest GCs were originated from a satellite system, very likely from the Large Magellanic Cloud (LMC). In such a case, age and metallicity can be decoupled, so the lowest-metallicity Galactic GCs are not necessarily the oldest component of the Milky Way. This is interesting because the Oosterhoff dichotomy among the Galactic GCs can be naturally reproduced by assuming that the lowest-metallicity GCs are slightly younger than the genuine Galactic GCs of similar metallicity.

Figure 5b conveys the essence of the Yoon & Lee (2002) explanation. The Galactic GCs are re-classified according to their Galactocentric distances (R_G), and shown along with the population models. From this figure, one can see that the inner- ($R_G < 8$ kpc) and outer-halo ($R_G > 8$ kpc) GCs are well represented by the models of the 13-Gyr population (solid line), and by those of a slightly younger population (11.8 Gyr; dashed line), respectively. The observed $\langle P_{ab} \rangle$ of the lowest-metallicity ($[\text{Fe}/\text{H}] < -2.0$) GCs are well reproduced by the dashed line. This line also fits the GCs on retrograde orbits, which are most likely an accreted component of the Milky Way (Zinn 1993; van den Bergh 1993). Note also that the LMC GCs follow the same dashed line. From this analysis, Yoon & Lee (2002) conclude that the Oosterhoff dichotomy can be viewed as a manifestation of the age structure of the Galactic GC system, and thus, of the Galactic assembly history.

Following the Yoon & Lee (2002) framework, we now compare the AMR and SHR models for NGC 6388 and NGC 6441 in terms of the $\langle P_{ab} \rangle$ vs. $[\text{Fe}/\text{H}]$ correlation (Fig. 5b). The use of the input parameters in Table 3 leads the AMR model to predict an $\langle P_{ab} \rangle$ that is too low at their $[\text{Fe}/\text{H}]$ (the lower stripe in Fig. 5b). This result is in line with Pritzl et al. (2002) and Catelan et al. (2003), who confirmed the difficulty in reproducing the RR Lyrae periods for the given metallicities of NGC 6388 and NGC 6441. We have explored a large parameter space to find a way to reproduce the observations of NGC 6388 and NGC 6441 based on the AMR assumption, but failed unless we assumed an unreasonably high age (> 17 Gyr). Such an unrealistically old age is not acceptable. Moreover, the very old population is predicted to have too few RR Lyrae stars when compared with the observations.

By contrast, the SHR model is remarkably consistent with the observations displayed in the Oosterhoff diagram (the upper stripe in Fig. 5b). We recall that all of the RR Lyraes belong to the blue-HB population in both the AMR and SHR models. When assuming that the helium abundance of the RR Lyraes is enhanced by $\Delta Y = 0.05$ (Table 3), their large $\langle P_{ab} \rangle$ values can be easily achieved at their $[\text{Fe}/\text{H}]$, even with RR Lyraes near the ZAHB. This is not surprising, since any effect that leads to a brighter HB such as an enhanced Y, would lead to longer periods, more consistent with the observations (Sweigart & Catelan

1998; Sweigart 1999).

We finish this section by discussing the unusual values of $N(c)/N(ab + c)$ of NGC 6388 and NGC 6441 for their metallicities. The combined data of NGC 6388 and NGC 6441 give 0.40 (= 34/85) (Corwin et al. 2006). The value falls between Oosterhoff group I (~ 0.2) and group II (~ 0.5). The c -type fraction of RR Lyrae variables has long been known to vary among GCs with differing HB types (Lee, Demarque, & Zinn 1990). The c -type fraction is significantly higher for predominantly blue HBs with little ZAHB stars within the RR Lyrae strip (Oosterhoff group II) than for red or intermediate HBs (group I). Lee, Demarque, & Zinn (1990) demonstrated that the evolutionary effect of blue HBs causes an uneven distribution in $(B - V)$, since the speed of evolution increases as a star evolves further from its original position. As a result, the GCs with predominantly blue HB components are predicted to have high incidences of bluer RR Lyraes, i.e., c -type variables. In this regard, the GCs with $0.3 \lesssim N(c)/N(ab + c) \lesssim 0.4$ can only be produced by a transitional HB morphology from intermediate-HB to predominantly-blue HBs. Under the normal-Y circumstances, GCs with such a transient HB type are rare, because it is hard for blue HBs to contain ZAHBs long enough to extend into the RR Lyrae strip. Few examples include NGC 5904 and NGC 6626 with $N(c)/N(ab + c) \sim 0.3$. By contrast, the SHR model can generate relatively easily blue HBs with long ZAHBs extending into the instability strip. This is because the high-Y HB tracks are characterized by considerably stretched blue loops (Sweigart 1987). The unusual value of $N(c)/N(ab + c)$ (~ 0.4) for NGC 6388 and NGC 6441, therefore, points toward the SHR scenario.

By means of the Oosterhoff class argument, we conclude that the SHR hypothesis provides a more plausible solution to the problem posed by the unusual behaviors of the RR Lyraes in NGC 6388 and NGC 6441. As suggested by Pritzl et al. (2000), NGC 6388 and NGC 6441 may be taken as a third class of Oosterhoff groups, and the helium abundance of RR Lyrae stars is the main driver behind this new class.

In this section, we have compared the two models in terms of RR Lyrae properties (i.e., the pulsating periods and the Oosterhoff classes), and consistently found that the observations are strongly in favor of the SHR scenario over the AMR scenario.

5. DISCUSSION

Using stellar population simulations, we have investigated the possibility that the bimodality of the HBs in NGC 6388 and NGC 6441 can be attributed to the presence of two distinct populations. This study was motivated by the discovery of multiple stellar popula-

tions coexisting in the most massive Galactic GC, ω Cen (Lee et al. 1999b; Standford et al. 2006, and references therein). We are particularly inspired by the fact that the integrated luminosities of NGC 6388, NGC 6441, and NGC 2808 (Harris 1996) make them *the 3rd, 5th, and 7th* brightest among the ~ 150 Galactic GCs (Yoon, Lee, & Lee 2000; Ree et al. 2002).

Two chemical enrichment scenarios for GCs are discussed; namely, the age-metallicity relation (AMR) and the super-helium-rich (SHR) scenarios. In both models, two hypothetical populations coexist within individual GCs. We have examined the CMD morphologies and the RR Lyrae properties of NGC 6388 and NGC 6441, and found consistently that the SHR scenario is superior to the AMR hypothesis in accounting for the observations. Our best solution is that the blue HB and the RR Lyrae stars are comprised of helium-enhanced ($\Delta Y \sim 0.05$) stars, which make up $\sim 15\%$ of the total population. Table 4 summarizes the model’s ability to reproduce various aspects of the observations.

Recently, Caloi & D’Antona (2007, hereafter CD07) have investigated the NGC 6441 HB population, including the periods of the RR Lyrae variables. From their analysis, CD07 conclude that $Y \simeq 0.35$ is required for the tilted red clump, $Y \simeq 0.37$ for the RR Lyrae stars, and $Y \simeq 0.38 - 0.40$ for the blue HB. A partial, qualitative agreement is found between our SHR model and CD07’s, in that the SHR population is necessarily invoked. However, several factors differentiate our result from CD07’s: (a) While our model assumes two discrete populations with distinct helium abundances, CD07 present a continuous distribution of helium content; (b) The helium abundance required in our SHR model to reproduce the blue HB is $Y \simeq 0.29 - 0.30$, which is well below the inferred Y in CD07 ($Y \simeq 0.35 - 0.40$); (c) Our model exhibits the tilted red clump naturally reproduced by the inclusion of differential reddening effect, thus indicating the red clumps of a normal helium abundance ($Y \simeq 0.24 - 0.25$). In short, the main difference lies in the predicted total helium abundance of the GCs, in that our SHR model requires significantly lower value of total helium abundance. CD07 predict the total helium-enriched population amounting to $\sim 60\%$ of the entire stellar content. We note that, as mentioned in §§ 3.3, the R-method argument by Layden et al. (1999) allows only a limited amount of helium content in the GCs. Furthermore, using deep *HST* photometry of NGC 6388, Catelan et al. (2006) discover the lack of a sizeable luminosity difference between the red HBs of NGC 6388 and 47 Tuc (a “flat”-red-clump GC with similar metallicity). This result points to the normal helium abundance of the red clump in NGC 6388, more consistent with our conclusion than CD07’s.

The high-helium hypothesis was originally suggested to explain the presence of hot EHBs by D’Antona et al. (2002). This notion has been expanded to account for the bimodal HBs found in NGC 2808 (D’Antona & Caloi 2004; Lee et al. 2005), NGC 6388, and NGC 6441 (D’Antona & Caloi 2004; D’Antona et al. 2005, 2006; Catelan 2005, CD07, this study). It is

noteworthy that the GCs with bimodal HBs often, if not always, also possess EHBs. Since the EHB phenomenon appears to share a common origin with HB bimodality, it is important to see whether the occurrence of EHBs correlates with GC mass, as does the instance of the bimodal HB (see Figure 1 of Lee, Gim, & Casetti-Dinescu (2007)). In fact, this was the basis for suggestions that the integrated luminosity plays an important role in the context of the second-parameter phenomenon (Fusi Pecci et al. 1993). Table 1 shows that eight Galactic GCs out of the 10 brightest contain hot EHB components (the 7th column). According to Catelan et al. (1998) catalog, $\sim 90\%$ (14 out of 16) of the EHB GCs have blue HBs. Given the fact that increasing metallicity makes an HB redder, we speculate that the EHB GCs with normal blue HBs in Table 1 (NGC 6266, NGC 7078, and NGC 6273) could have typical *bimodal* HBs if they were as metal-rich as NGC 6388 and NGC 6441.

Several mechanisms have been proposed to explain the peculiar chemical history of GCs with helium-excess populations (D’Antona et al. 2002; Ventura et al. 2001, 2002; Norris 2004; Gratton, Sneden, & Carretta 2004; Bekki & Norris 2006; Chuzhoy 2006; Choi & Yi 2007; Tsujimoto, Shigeyama, & Suda 2007; Newsham & Terndrup 2007). One theoretical requirement for the proposed chemical evolution is an initially high mass to retain the ejecta of the first generation stars, as is evident in the case of ω Cen (Norris 2004; Piotto et al. 2005; Lee et al. 2005; Bekki & Norris 2006). The HB bimodality found in massive GCs such as NGC 6388, NGC 6441 (D’Antona & Caloi 2004; D’Antona et al. 2005, 2006; Catelan 2005, CD07, this study), and NGC 2808 (D’Antona & Caloi 2004; Lee et al. 2005; Piotto et al. 2007) appears to be another piece of evidence for a link between the GC mass and the helium-enrichment process. It has been suggested that ω Cen was once part of a more massive system that later merged with the Milky Way (Lee et al. 1999b; Dinescu 2002; Altmann, Catelan, & Zoccali 2005; Meza et al. 2005; Bekki & Norris 2006, and references therein). Similar accretion events may have continued throughout the Galactic history, and the massive GCs with bimodal HB distributions may be considered minor versions of ω Cen, representing relics of the Galaxy assembly process (see Lee, Gim, & Casetti-Dinescu (2007) for further discussion).

Another important implication of our results concerns the long-standing second parameter debate regarding HB morphology. Given that the HB-bimodality phenomenon has long been taken as the strongest evidence against the GC age being the second parameter, a fully satisfactory solution will not be found until the origin of the HB bimodality has been accounted for. Our results suggest that the GC-to-GC variation in helium abundance, which was one of the first candidates for the second parameter in the literature (Sandage & Wildey 1967; van den Bergh 1967), have a role in giving rise to the HB bimodality. If our interpretation is confirmed, the GC-to-GC helium variation found most often in massive GCs should be considered a *local* effect rather than a global one, further supporting age as the

global second parameter. Further observations and modelling of GCs with bimodal HBs are still required to verify that helium variation is a local effect, and thus the third parameter controlling HB morphology.

We would like to thank Michael Rich for providing the observational data in Figures 2 & 3. Helpful comments from the referee were gratefully appreciated. S.-J. Y. acknowledges support from the Basic Research Program of the Korea Science & Engineering Foundation (Grant No. R01-2006-000-10716-0), and from the Korea Research Foundation Grant (MOEHRD: KRF-2006-331-C00134).

REFERENCES

- Altmann, M., Catelan, M., & Zoccali, M. 2005, *A&A*, 439, 5
- Anderson, J. 2002, in ω Centauri, a Unique Window into Astrophysics, ASP Conf. Ser. 265, eds F. van Leeuwen, J. D. Hughes, and G. Piotto. (San Francisco: ASP), p. 87
- Armandroff, T. E., & Zinn, R. 1988, *AJ*, 96, 92
- Beaulieu, S. F., et al. 2001, *AJ*, 121, 2618
- Bedin, L. R., Piotto, G., Anderson, J., Cassisi, S., King, I. R., Momany, Y., & Carraro, G. 2004, *ApJ*, 605, L125
- Bekki, K., & Norris J. E. 2006, *ApJ*, 637, L109
- Bellazzini, M., Ferraro, F. R., & Buonanno, R. 1999, *MNRAS*, 307, 619
- Bellazzini, M., Fusi Pecci, F., Ferraro, F. R., Galletti, S., Catelan, M., & Landsman, W. B. 2001, *AJ*, 122, 2569
- Brown, T. M., Sweigart, A. V., Lanz, T., Landsman, W. B., & Hubeny, I. 2001, *ApJ*, 562, 368
- Busso, G., Piotto, G., & Cassisi, S. 2004, *Mem. Soc. Astron. Italiana*, 75, 46
- Caloi, V., & D’Antona, F. 2007, *A&AS*, 463, 949 (CD07)
- Castellani, V., & Quarta, M. L. 1987, *A&AS*, 71, 1
- Catelan, M. 2000, *ApJ*, 531, 826

- Catelan, M. 2005, in Resolved Stellar Populations, ASP Conf. Ser., ed. D. Valls-Gabaud & M. Chavez, *in press* (asto-ph/0507464)
- Catelan, M., et al. 2006, ApJ, 651, L133
- Catelan, M., Borissova, J., Sweigart, A. V., & Spassova, N. 1998, ApJ, 494, 265
- Catelan, M., & de Freitas P. 1996, PASP, 108, 166
- Catelan, M., Sweigart, A. V., Pritzl, B. J., & Smith, H. A. 2003, in New Horizons in Globular Cluster Astronomy, ASP Conf. Ser. 296, eds. Giampaolo Piotto, Georges Meylan, S. George Djorgovski and Marco Rielo (San Francisco: ASP), p. 289
- Choi, E., & Yi, S. K. 2007, MNRAS, 375, L1
- Chuzhoy, L. 2006, MNRAS, 369, L52
- Clement, C., et al. 2001, AJ, 122, 2587
- Clementini, G., et al. 2005, ApJ, 630, L145
- Corwin, T. M., Sumerel, A. N., Pritzl, B. J., Smith, H. A., Catelan, M., Sweigart, A. V., & Stetson, P. B. 2006, AJ, 132, 1014
- D’Antona, F., Bellazzini, M., Caloi, V., Pecci, F. F., Galleti, S., & Rood, R. T. 2005, ApJ, 631, 868
- D’Antona, F., & Caloi, V. 2004, ApJ, 611, 871
- D’Antona, F., Caloi, V., Montalbán, J., Ventura, P., & Gratton, R. 2002, A&A, 395, 69
- D’Antona, F., Ventura, P., & Caloi, V. 2006, Mem. Soc. Astr. It., 77, 168
- Dinescu, D. I. 2002, in ω Centauri, a Unique Window into Astrophysics, ASP Conf. Ser. 265, eds F. van Leeuwen, J. D. Hughes, and G. Piotto. (San Francisco: ASP), p. 365
- Fusi Pecci, F., Ferraro, F. R., Bellazzini, M., Djorgovski, S., Piotto, G., & Buonanno, R. 1993, AJ, 105, 1145
- Gratton, R. G., et al. 2007, A&A, 464, 953
- Gratton, R. G., Sneden, C., & Carretta, E. 2004, ARA&A, 42, 385
- Harris, W. E. 1996, AJ, 112, 1487

- Heitsch, F., & Richtler, T. 1999, *A&A*, 347, 455
- Hilker, M., & Richtler, T. 2000, *A&A*, 362, 895
- Kim, Y.-C., Demarque, P., Yi, S. K., & Alexander, D. R. 2002, *ApJS*, 143, 499
- Law, D. R., Majewski, S. R., Skrutskie, M. F., Carpenter, J. M., & Ayub, H. F. 2003, *AJ*, 126, 1871
- Layden, A. C., & Sarajedini, A. 2000, *AJ*, 119, 1760
- Layden, A. C., Ritter, L. A., Welch, D. L., & Webb, T. M. A. 1999, *AJ*, 117, 1313
- Lee, H.-c., Yoon, S.-J., & Lee, Y.-W. 2000, *AJ*, 120, 998
- Lee, Y.-W., et al. 2005, *ApJ*, 621, L57
- Lee, Y.-W., Demarque, P., & Zinn, R. 1990, *ApJ*, 350, 155
- Lee, Y.-W., Demarque, P., & Zinn, R. 1994, *ApJ*, 423, 248
- Lee, Y.-W., Gim, H. B., & Casetti-Dinescu, D. I. 2007, *ApJ*, 661, L49
- Lee, Y.-W., Joo, J.-M., Sohn, Y.-J., Rey, S.-C., Lee, H.-C., & Walker, A. R. 1999b, *Nature*, 402, 55
- Lee, Y.-W., Yoon, S.-J., Lee, H.-C., & Woo, J.-H. 1999a, in *Spectrophotometric Dating of Stars and Galaxies*, ASP Conf. Ser. 192, eds. Ivan Hubeny, Sally Heap, and Robert Cornett (San Francisco, ASP), p. 185
- Lee, Y.-W., & Zinn, R. 1990, in *Confrontation between Stellar Pulsation and Evolution*, ASP Conf. Ser. 11 (San Francisco, ASP), p. 26
- Lanz, T., Brown, T. M., Sweigart, A., Hubeny, I., & Landsman, W. B. 2004, *ApJ*, 602, 342
- Lejeune, T., Cuisinier, F., & Buser, R. 1998, *A&AS*, 130, 65
- Meza, A., Navarro, J. F., Abadi, M. G., & Steinmetz, M. 2005, *MNRAS*, 359, 93
- Moehler, S., & Sweigart, A. V. 2006, *A&A*, 455, 943
- Moehler, S., Sweigart, A. V., Landsman, W. B., Hammer, N. J., & Dreizler, S. 2004, *A&A*, 415, 313
- Newsham, G., & Terndrup, D. M. 2007, *ApJ*, 664, 332

- Norris, J. E. 2004, *ApJ*, 612, L25
- Oosterhoff, P. T. 1939, *Observatory*, 62, 104
- Pancino, E., Ferraro, F. R., Bellazzini, M., Piotto, G., & Zoccali, M. 2000, *ApJ*, 534, L83
- Park, J.-H. & Lee, Y.-W. 1997, *ApJ*, 476, 28
- Piotto, G., et al. 1997, in *Advances in Stellar Evolution*, eds. R. T. Rood and A. Renzini (Cambridge: Cambridge Univ. Press), p.84
- Piotto, G., et al. 2005, *ApJ*, 621, 777
- Piotto, G., Bedin, L. R., Anderson, J., King, I. R., Cassisi, S., Milone, A. P., Villanova, S., Pietrinferni, A., & Renzini, A. 2007, *ApJ*, 661, L53
- Piotto, G., King, I. R., Djorgovski, S. G., Sosin, C., Zoccali, M., Saviane, I., De Angeli, F., Riello, M., Recio Blanco, A., Rich, R. M., Meylan, G., & Renzini, A. 2002, *A&A*, 391, 945
- Pritzl, B., Smith, H. A., Catelan, M., & Sweigart, A. V. 2000, *ApJ*, 530, L41
- . 2001, *AJ*, 122, 2600
- . 2002, *AJ*, 124, 949
- Pritzl, B., Smith, H. A., Stetson, P. B., Catelan, M., Sweigart, A. V., Layden, A. C., & Rich, R. M. 2003, *AJ*, 126, 1381
- Raimondo, G., Castellani, V., Cassisi, S., Brocato, E., & Piotto, G. 2002, *ApJ*, 569, 975
- Recio-Blanco, A., Aparicio, A., Piotto, G., De Angeli, F., & Djorgovski, S. G. 2006, *A&A*, 452, 875
- Ree, C. H., Yoon, S.-J., Rey, S.-C., & Lee, Y.-W. 2002, in *Omega Centauri: A Unique Window into Astrophysics*, ASP Conf. Ser. 265, ed. F. van Leeuwen, G. Piotto, and J. Hughes (San Francisco, ASP), p. 101
- Reimers, D. 1975, in *Mem. Soc. R. Sci. Liège 6 Sér.*, 8, 369
- Rey, S.-C., Yoon, S.-J., Lee, Y.-W., Chaboyer, B., & Sarajedini, A. 2001, *AJ*, 122, 3219
- Rich, R. M., et al. 1997, *ApJ*, 484, L25
- Rood, R. T. 1970, *ApJ*, 161, 145

- Rood, R. T., et al. 1993, in *The Globular Clusters-Galaxy Connection*, ASP Conf. Ser. 48, eds. G. H. Smith and J. P. Brodie (San Francisco, ASP), p. 218
- Rosenberg, A., Recio-Blanco, A., & García-Marín, M. 2004, *ApJ*, 603, 135
- Sandage, A., & Wildey, R. 1967, *ApJ*, 150, 469
- Sarajedini, A., Chaboyer, B., & Demarque, P. 1997, *PASP*, 109, 1321
- Siegel, M. H., et al. 2007, *ApJ*, 667, L57
- Sosin, C., Dorman, B., Djorgovski, S. G., Piotto, G., Rich, R. M., King, I. R., Liebert, J., Phinney, E. S., & Renzini, A. 1997, *ApJ*, 480, L35
- Stanford, L. M., Da Costa, G. S., Norris, J. E., & Cannon, R. D. 2006, *ApJ*, 647, 1075
- Stetson, P. B., Vandenberg, D. A., & Bolte, M. 1996, *PASP*, 108, 560
- Sweigart, A. V. 1987, *ApJS*, 65, 95
- Sweigart, A. V. 1999, in *Spectrophotometric Dating of Stars and Galaxies*, ASP Conf. Ser., Vol. 192, ed. I. Hubeny, S. R. Heap, & R. H. Cornett (San Francisco: ASP), 239
- Sweigart, A. V., & Catelan, M. 1998, *ApJ*, 501, L63
- Sweigart, A. V., & Gross, P. G. 1976, *ApJS*, 32, 367
- Tsujimoto, T., Shigeyama, T., & Suda, T. 2007, *ApJ*, 654, L139
- van den Bergh, S. 1967, *AJ*, 72, 70
- van den Bergh, S. 1993, *AJ*, 105, 971
- van den Bergh, S. 1996, *ApJ*, 471, L31
- Ventura, P., D’Antona, F., & Mazzitelli, I. 2002, *A&A*, 393, 215
- Ventura, P., D’Antona, F., Mazzitelli, I., & Gratton, R. 2001, *ApJ*, 550, L65
- Yoon, S.-J., Lee, C.-H., & Lee, Y.-W. 2000, *BAAS*, 196, 41.02
- Yoon, S.-J., & Lee, Y.-W. 2002, *Science*, 297, 578
- Yoon, S.-J., Yi, S. K., & Lee, Y.-W. 2006, *Science*, 311, 1129

Zinn, R. 1993, in *The Globular Clusters-Galaxy Connection*, ASP Conf. Ser. 48, eds. G. H. Smith and J. P. Brodie (San Francisco, ASP), p. 38

Table 1. The 10 Brightest Galactic Globular Clusters and the Features in their CMDs

Rank	NGC	Name	M_V^{tot} ^a	[Fe/H] ^b	Composite CMD ^c ?	HB Shape	References
1	5139	ω Cen	-10.29	-1.59	Yes (Multiple MS/HB/RGB)	Multiple HB + EHB	1, 2, 3, 4
2	6715	M54	-10.01	-1.43	Yes (Multiple RGB/HB)	Multiple HB + EHB	5, 6, 7
3	6388	...	-9.82	-0.60	Yes (Bimodal HB)	Bimodal HB + EHB	8, 9, 10
4	2419	...	-9.58	-2.10	No	Normal blue HB	8
5	6441	...	-9.47	-0.53	Yes (Bimodal HB)	Bimodal HB + EHB	8, 9, 11
6	104	47 Tuc	-9.42	-0.71	No	Normal red HB	9
7	2808	...	-9.36	-1.37	Yes (Multiple MS/HB)	Bimodal HB + EHB	9, 12, 13
8	6266	M62	-9.19	-1.29	No	Long blue HB + EHB	9
9	7078	M15	-9.17	-2.17	No	Normal blue HB + EHB	9
10	6273	M19	-9.08	-1.68	No	Normal blue HB + EHB	9

^a M_V^{tot} is obtained from Harris (1996).

^b[Fe/H] is obtained from Zinn (1993).

^cCMDs with multiple RGBs and/or HBs.

References. — (1) Lee et al. (1999b); (2) Hilker & Richtler (2000); (3) Pancino et al. (2000); (4) Piotto et al. (2005); (5) Bellazzini et al. (1999); (6) Layden & Sarajedini (2000); (7) Rosenberg et al. (2004); (8) Rich et al. (1997); (9) Piotto et al. (2002); (10) Catelan et al. (2006); (11) Pritzl et al. (2003); (12) Sosin et al. (1997); (13) Piotto et al. (2007)

Table 2. Model Ingredients

Ingredient	Stellar & Flux Libraries
MS to RGB Evolutionary Tracks	Kim et al. (2002) Yonsei–Yale Normal-helium Isochrones Kim et al. (2008, <i>in prep.</i>) Yonsei–Yale Helium-rich Isochrones
Post-RGB Evolutionary Tracks .	Han et al. (2008, <i>in prep.</i>) Yonsei–Yale Normal-helium HB Tracks Han et al. (2008, <i>in prep.</i>) Yonsei–Yale Helium-rich HB Tracks
Flux Library	Lejeune, Cuisinier, & Buser (1998) Model Atmosphere
RR Lyrae Variable Stars	Lee, Demarque, & Zinn (1990) Prescriptions

Table 3. Model Input Parameters

Parameter	NGC 6388	NGC 6441
Common Parameters:		
Initial mass function	Salpeter	Salpeter
α -element enhancement, $[\alpha/\text{Fe}]$	0.3	0.3
Distance modulus, $(V - M_V)$ (mag.)	16.50	17.17
Galactic reddening, $E(B - V)$ (mag.)	0.34	0.43
Differential reddening, $\sigma_{E(B-V)}$ (mag.)	0.03	0.03
Extinction coefficient, $A_V/E(B - V)$	3.1	3.1
HB mass dispersion, $\sigma_M (M_\odot)$	0.02	0.02
RR Lyrae instability strip width, $\Delta \text{Log } T_e$ (K)	0.085	0.085
Reimers' (1975) mass-loss efficiency parameter, η	0.56	0.56
The AMR Model^a:		
Metal abundance, Z	0.007 & 0.0035	0.008 & 0.0055
Helium abundance, Y	0.245 & 0.245	0.245 & 0.245
Absolute age, t (Gyr)	13.0 & 15.0	13.0 & 15.0
Number fraction (%)	82 & 18	86 & 14
The SHR Model^b:		
Metal abundance, Z	0.007 & 0.007	0.008 & 0.008
Helium abundance, Y	0.245 & 0.295	0.245 & 0.295
Absolute age, t (Gyr)	13.0 & 13.0	13.0 & 13.0
Number fraction (%)	82 & 18	86 & 14

^aMetal-rich younger & metal-poor older populations

^bNormal-helium & helium-enriched populations

Table 4. Summary of Model Ability to Reproduce Observations

Feature	The AMR Model	The SHR Model
Single RGB	○	○
RGB Bump Luminosity	○	○
RGB Bump Slope	○	○
HB Bimodality	○	○
Red HB Tilt	○	○
Overall HB Slope	×	○
Extreme HB	×	△
RR Lyrae Luminosity ..	×	○
RR Lyrae Period	×	○
$N(c)/N(ab + c)$	○	○
Oosterhoff Diagram	×	○

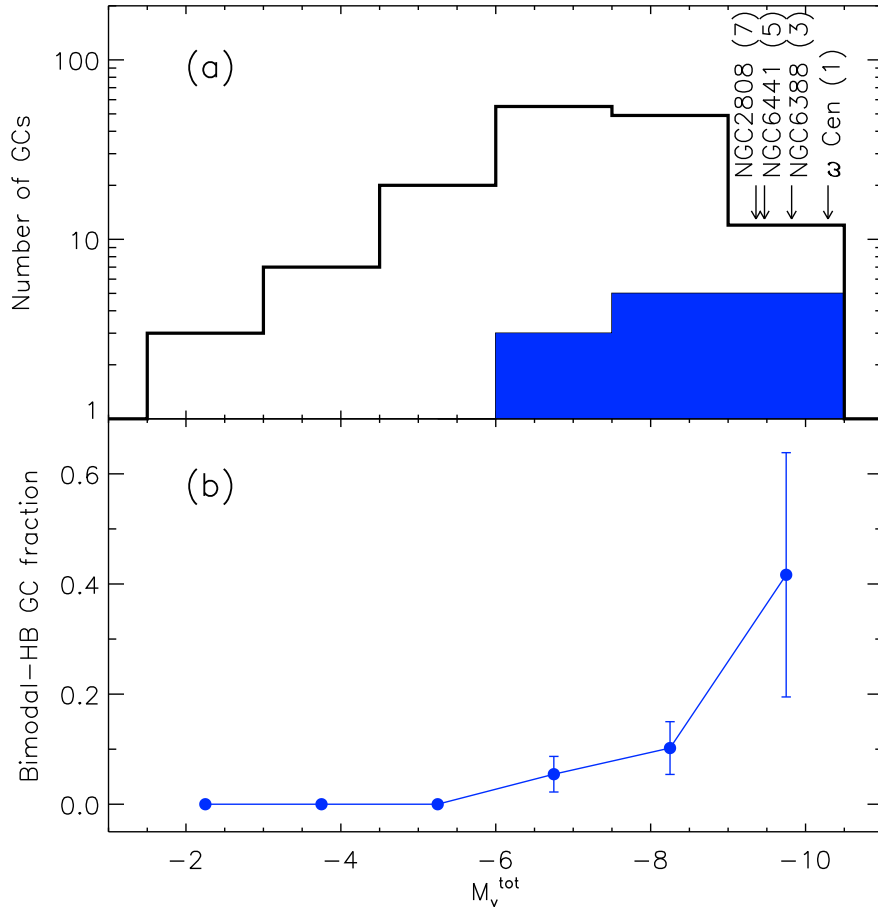


Fig. 1.— (a) The V -band luminosity function (open histogram) of 147 Galactic GCs from Harris (1996) catalog. Arrows denote the integrated magnitude of the brightest GC, ω Cen, and the GCs with bimodal HBs among the 10 brightest GCs. The numbers in the parentheses denote their brightness ranks. NGC 6388 and NGC 6441 are among the most massive GCs. The filled histogram is for the 11 bimodal-HB GCs (Catelan et al. 1998) plus ω Cen and M54. Note that they are all brighter than $M_V^{tot} \simeq -7$. (b) The relative number fraction of bimodal-HB GCs plus ω Cen and M54 as a function of the integrated magnitude. Their fraction in a luminosity bin increases with increasing luminosity. Error bars show Poisson errors.

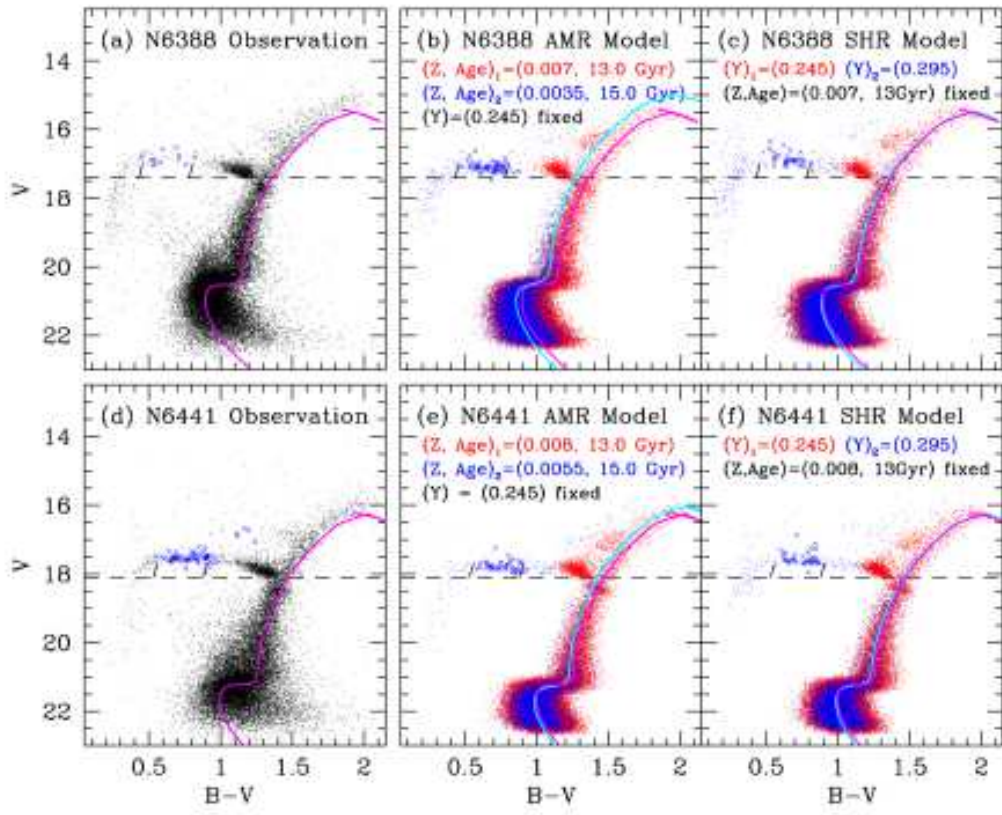


Fig. 2.— Comparison of the observational data (*a* & *d*) with the AMR model (*b* & *e*) and the SHR model (*c* & *f*) for NGC 6388 and NGC 6441. (*a* & *d*) The observed CMDs are from Rich et al. (1997). Isochrones are overlaid with observations, from which the dominant major populations, i.e., the metal-rich younger population in the AMR model and the normal-helium population from the SHR model, are generated. Crosses represent the observed RR Lyrae stars from Pritzl et al. (2001, 2002, 2003). The same RR Lyrae stars are also shown in Fig. 4. Horizontal dashed lines represent the brightness at the base of red clumps. Short tilted solid lines denote the RR Lyrae instability strips. (*b*, *c*, *e*, & *f*) In *b* & *e*, the metal-rich younger (denoted by “1”) and the metal-poor older (denoted by “2”) populations are respectively shown as red and blue dots. The magenta and cyan isochrones are respectively for the metal-rich younger and the metal-poor older populations. The combinations of metallicity, helium abundance, and age required to reproduce the CMD morphology are denoted. Note that the observed bimodal HBs are explained as the sum of the red HBs from component 1 (red dots) and the blue HBs from component 2 (blue dots). Crosses denote the model RR Lyrae stars. In *c* & *f*, the normal-helium (denoted by “1”) and the helium-excess (denoted by “2”) populations are respectively shown as red and blue dots. The magenta and cyan isochrones are respectively for the normal-helium and the helium-excess populations. Note that the observed bimodal HBs are explained as the sum of red HBs from component 1 (red dots) and blue HBs from component 2 (blue dots). Crosses denote the model RR Lyrae stars.

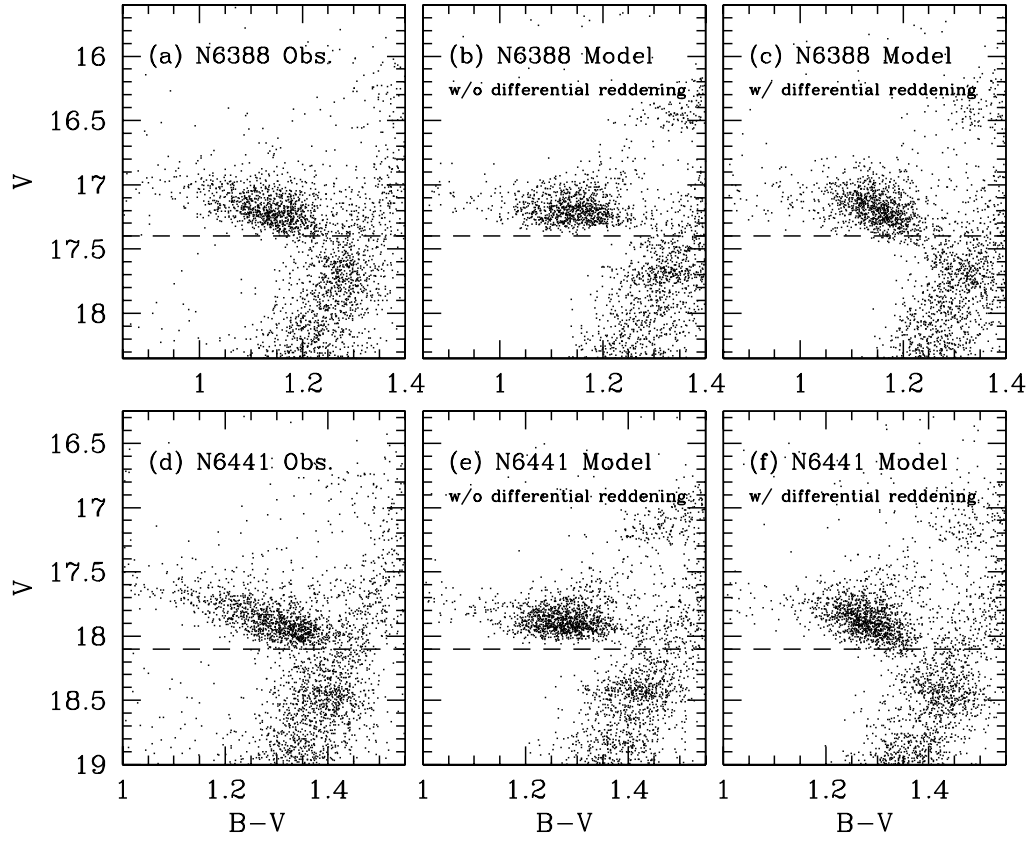


Fig. 3.— Numerical experiments on the effect of differential reddening on the red clumps. The observed clumps (*a* & *d*) are compared with the flat clumps generated without the differential reddening effect (*b* & *e*), and the tilted clumps generated with the effect (*c* & *f*). Note that panels (*a* & *d*) and (*c* & *f*) are identical to Figs. 2*a* & 2*d* and Figs. 2*c* & 2*f*, but have been magnified around the HB red clump region. The dominant major population is common across the AMR (the metal-rich younger component denoted by “1” in Fig. 2) and SHR (the normal-helium component denoted again by “1” in Fig. 2) models. The inferred differential reddening appears to be enough to turn a “normal” red HB component into a significantly sloped structure. Note also that the differential reddening effect appears to be necessary to reproduce the observed scatter and the possible tilt of the RGB bumps.

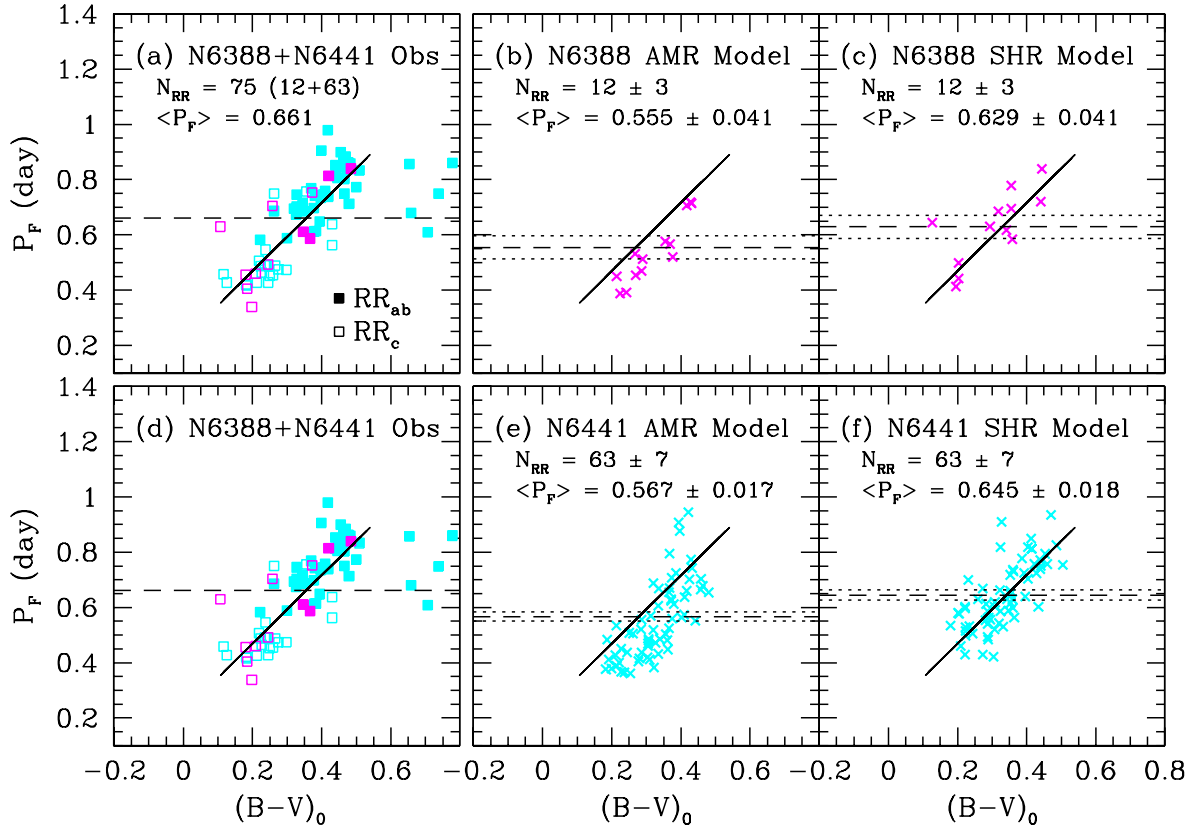


Fig. 4.— Comparison of the observations (*a* & *d*) with the AMR model (*b* & *e*) and the SHR model (*c* & *f*) for NGC 6388 and NGC 6441 in the $(B-V, \langle P_F \rangle)$ plane. (*a* & *d*) The observed RR Lyrae variables are from Pritzl et al. (2001, 2002, 2003). Solid and open squares represent *ab*-type and *c*-type RR Lyrae stars, respectively. Type *c* RR Lyrae were fundamentalized by $\text{Log } P_F = \text{Log } P_c + 0.13$ (Castellani & Quarta 1987; Lee, Demarque, & Zinn 1990). In order to avoid small number statistics, the catalogs of NGC 6388 (12 RR Lyraes from Pritzl et al. (2002)) and NGC 6441 (63 RR Lyraes from Pritzl et al. (2001, 2003)) were combined. Dashed line in (*a*) denotes the observed mean P_F value ($\langle P_F \rangle = 0.661$ day) for the combined NGC 6388 (magenta) and NGC 6441(cyan) data. Solid line is the least-squares fit to the data. Panel (*d*) is identical to panel (*a*). (*b*, *c*, *e*, & *f*) Examples of the Monte Carlo simulations. Solid lines are the same as in (*a* & *d*). Dashed and dotted lines in (*b* & *e*) and (*c* & *f*) denote the mean values of P_F and their 1σ uncertainties of 10,000 synthetic simulations for the AMR model and the SHR model, respectively.

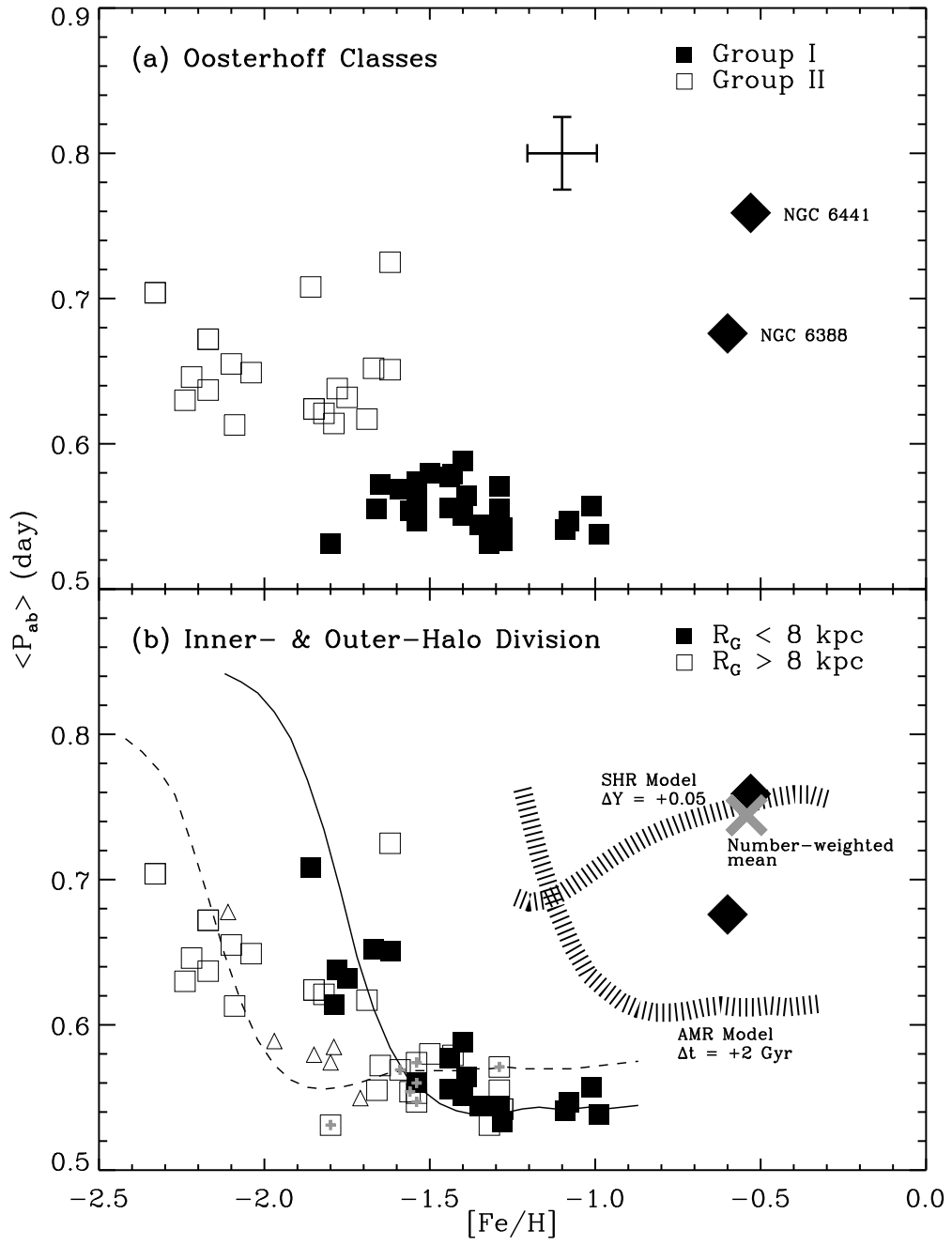


Fig. 5.— (a) Oosterhoff classes. The correlation between the mean period of type ab RR Lyraes ($\langle P_{ab} \rangle$) and $[\text{Fe}/\text{H}]$ for GCs in the Galaxy is shown. The data are from Clement et al. (2001). GCs having 5 or more type ab RR Lyraes are shown. The error bar denotes the mean errors. GCs are mainly divided into two distinct groups according to the mean period and the metal abundance: Oosterhoff group I (filled squares; $\langle P_{ab} \rangle \simeq 0.55$ days, and $[\text{Fe}/\text{H}] > -1.8$) or group II (open squares; $\langle P_{ab} \rangle \simeq 0.65$ days, and $[\text{Fe}/\text{H}] < -1.6$). The $\langle P_{ab} \rangle$ values for NGC 6388 (0.676 days from nine type- ab variables) and for NGC 6441 (0.759 days from 42 type- ab variables) are obtained from Corwin et al. (2006). Note that NGC 6388 and NGC 6441 (solid diamonds) belong to neither Oosterhoff group. (b) Inner- & outer-halo division. Solid and dashed lines are our model predictions for the 13-Gyr and 11.8-Gyr populations, respectively. GCs with the Galactocentric distance, $R_G < 8$ kpc (filled squares) are well reproduced by the models for the old population (solid line), whereas most GCs with $R_G > 8$ kpc (open squares) follow the model locus for slightly younger ages (dashed line). Small plus signs mark GCs on retrograde orbits around the Galactic center, whereas triangles represent the old GCs found in the LMC halo. Note that the retrograding GCs and the LMC GCs follow the dashed line. Large gray cross between the diamonds marks the number-weighted mean values of $[\text{Fe}/\text{H}]$ and $\langle P_{ab} \rangle$ for NGC 6388 and NGC 6441. Two thick stripes indicate the AMR model ($\Delta t = +2$ Gyr, lower stripe) and the SHR model ($\Delta Y = +0.05$, upper stripe). Note that the SHR model prediction succeeds in reproducing the unusual positions of NGC 6388 and NGC 6441.